

---

## Basic Study on Solid-Liquid Phase Change Problem of Ice around Heat Transfer Tubes

### - Freezing Phenomenon and Prediction of Bridging Time around Two Elliptical Tubes -

Qiang-Sheng WANG<sup>1</sup>, Koichi HIROSE<sup>2</sup> and Takashi FUKUE<sup>3</sup>

<sup>1</sup> Department of Mechanical Engineering, Civil and Environmental Engineering, Graduate School of Iwate University, Morioka, Iwate 020-8551, Japan

<sup>2,3</sup> Department of Systems Innovation Engineering, Iwate University, Morioka, Iwate 020-8551, Japan

---

**Abstract:-** Phase change heat transfer around heat transfer tubes is one of the basic problem of an ice heat storage exchanger. It can lead to decrease of thermal storage efficiency and damage of heat transfer tubes if continued freezing further after the ice has bridged because of the generated ice thermal resistance and volume expansion. In this study, we focused on freezing phenomena of phase change material (PCM) between two heat transfer tubes, which can simulate an inside structure of ice heat storage exchangers. Bridging time between two heat transfer tubes was studied numerically. We used water as the PCM, which is filled in the water container. Two horizontal elliptical tubes were used as heat transfer tubes in order to observe the influence of natural convection. Single-domain calculation model was used to calculate arbitrary shape of the two tubes during the ice freezing process. We changed arranged angle and relative position of the tubes to investigate impact of the tube arrangement on freezing phenomenon. In order to confirm the accuracy of our analysis, analytical results were compared with experimental results at the same conditions. Results show that the bridging time was not simply in proportional to the initial temperature of water when considered the natural convection influenced by such as density inversion of water. Moreover, we found that when we set the temperature of tube wall and initial temperature of water as the parameters, bridging time has a similar trend with distance between the axes. Therefore, it is possible to predict the bridging time for elliptical heat transfer tube.

**Keywords:-** Freezing phenomena, Natural convection, Bridging time, Temperature distribution, Numerical prediction

---

### 1. INTRODUCTION

Latent heat storage system is one of the apparatus that use absorption and release of the large latent heat when the PCM is freezing and thawing. There are many researches have been studied on the latent heat storage system. Saito, Sasaguchi and J. Vogel [1-4] et al. clarified the effect of natural convection and density inversion to latent heat storage system. Torigoe [5] et al. researched the effects of tube numbers and arrangement on the liquid phase change process. Hirose et al. analysed the characteristic of phase change heat transfer around horizontal tubes immersed in water [6-8]. Moreover, T.J. Scanlon [9] et al. investigated the melting-freezing problem in rectangular container. Casano [10] et al. did an experimental and numerical investigation of the steady periodic solid-liquid phase change heat transfer. Recently, Longeon [11] et al. studied influence of the natural convective heat transfer mechanism during the phase transition processes. Kozak [12] et al. found that a vertical double pipe concentric storage unit with the circumferentially finned inner tube can significantly enhance the melting process.

As for the PCM, water is being used in many cases because its latent heat is about 80 times of its sensible heat. Therefore, reduction of the thermal storage space could be realized by storing the cold heat as ice. Generally, ice thermal storage system can be roughly divided into static and dynamic type. And for the static type, we know that it could cause damage to tube group and decrease of heat storage efficiency if continued freezing after the ice has been bridged because of the generated ice thermal resistance and volume expansion. This is also one of the important factors that prevent the compactification and high performance of the system. However, researches on bridging phenomenon after the ice bridged with each other have rarely been reported. Therefore, prediction of bridging time is important for improving the efficiency of ice heat storage device.

In this study, we focused on the bridging phenomenon between heat transfer tubes and the aim of this study is to investigate the feasibility of an estimated bridging time. The freezing phenomenon and bridging time was studied numerically and experimentally. As a step of exploration, we set several parameters such as the tube temperature and initial water temperature to observe the changes of freezing phenomenon and the bridging time.

## 2. ANALYTICAL AND EXPERIMENTAL METHOD

### 2.1 Physical Model and Coordinate System

Physical model and coordinate system of the two elliptical tubes used in this study are shown in Fig.1. We assumed that the horizontally arranged tubes were placed in a region full filled with water and the frozen layer was around the tubes with coolant flowing inside of the tubes. The growth of the frozen layer around the heat transfer tube will begin at the moment when the tubes are being cooled.

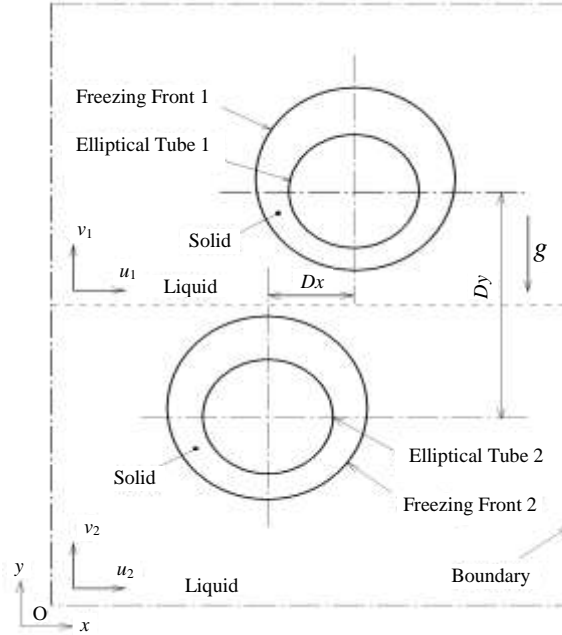


Fig.1 Physical model and coordinate systems.

One-dot chain line in the figure shows the surrounding border which represents the calculation region and the broken line is a part connecting the upper and lower calculation areas so that the movement of flow and temperature could connect smoothly. The coordinate system is a Cartesian coordinate system with the Origin on the lower left of the calculation area.

The following assumptions were introduced in our analysis:

- (1) The flow is uncompressed two-dimensional laminar flow.
- (2) The density of liquid can be changed only by buoyancy term.
- (3) There is no change in volume due to the phase change.
- (4) Super cooling phenomenon does not occur.

The derivation and discretization of basic equations were carried out by using the above assumptions.

### 2.2 Governing Equations

The governing equations in Cartesian coordinate system (  $x, y$  ) was converted to equations in the general coordinate system (  $\xi, \eta$  ) by using the boundary fitted coordinate method which can set the boundary condition along any tubular shape when analyzing the flow around the tube. Governing equations of the two-dimensional Cartesian coordinate system are shown in the following:

Continuity equation:

$$\frac{\partial u}{\partial x} + \frac{\partial v}{\partial y} = 0 \quad (1)$$

Equation of motion in the x-direction:

$$\frac{\partial u}{\partial t} + u \frac{\partial u}{\partial x} + v \frac{\partial u}{\partial y} = -\frac{1}{\rho} \frac{\partial p}{\partial x} + \nu \left( \frac{\partial^2 u}{\partial x^2} + \frac{\partial^2 u}{\partial y^2} \right) \quad (2)$$

Equation of motion in the y-direction:

$$\frac{\partial v}{\partial t} + u \frac{\partial v}{\partial x} + v \frac{\partial v}{\partial y} = -\frac{1}{\rho} \frac{\partial p}{\partial y} + \nu \left( \frac{\partial^2 v}{\partial x^2} + \frac{\partial^2 v}{\partial y^2} \right) + b_y \quad (3)$$

Energy equation:

$$\frac{\partial T}{\partial t} + u \frac{\partial T}{\partial x} + v \frac{\partial T}{\partial y} = a \left( \frac{\partial^2 T}{\partial x^2} + \frac{\partial^2 T}{\partial y^2} \right) \quad (4)$$

Where,  $b_y$  represents the buoyancy term,  $a$  represents the thermal diffusivity and  $a = \lambda / \rho c_p$ .

The governing equations converted by the general variable  $f$  according to the general coordinate system are shown in the following:

$$J \frac{\partial f}{\partial t_o} + \frac{\partial}{\partial \xi}(Uf) + \frac{\partial}{\partial \eta}(Vf) - \frac{\partial}{\partial \xi} \{ \Gamma J (q_{11} f_\xi + q_{12} f_\eta) \} - \frac{\partial}{\partial \eta} \{ \Gamma J (q_{21} f_\xi + q_{22} f_\eta) \} = J \cdot S(\xi, \eta) \quad (5)$$

Operators in the above equations are defined as the following:

$$q_{11} = \xi_x^2 + \xi_y^2, \quad q_{12} = \xi_x \eta_x + \xi_y \eta_y, \quad \eta_{y21} = q_{12}, \quad q_{22} = \eta_x^2 + \eta_y^2, \quad J = x_\xi y_\eta - x_\eta y_\xi \quad (6)$$

$S, f, \Gamma$  in the above equations except the continuity equation are corresponding to the following:

Equation of motion,

$x$  - direction:

$$f = u, \Gamma = v, S = -\frac{1}{\rho} \left( \xi_x \frac{\partial p}{\partial \xi} + \eta_x \frac{\partial p}{\partial \eta} \right) \quad (7)$$

$y$  - direction:

$$f = v, \Gamma = v, S = -\frac{1}{\rho} \left( \xi_y \frac{\partial p}{\partial \xi} + \eta_y \frac{\partial p}{\partial \eta} \right) + g\beta(T - T_\infty)B(T) \quad (8)$$

Energy equation:

$$f = T, \Gamma = a, S = 0 \quad (9)$$

### 2.3 Boundary Condition

As initial conditions in the analysis, liquid phase was assumed to be stationary at water temperature of  $T = T_{ini}$  and the temperature of tube wall as boundary condition was set at  $T = T_w$  at the beginning. Additionally, the surface of heat transfer tube was at no slip condition as for the analysis of flow. One-dot chain line in the schematic diagram shown in Fig.1 represents the boundary (which was considered as the adiabatic wall) of computational domain and in this paper we also set it at no slip condition. Physical properties used for the analysis are described in the physical property book of heat transfer engineering materials [13]. However, the Fujii's expression [14] as shown in Fig.2 was used as the relationship between water temperature and density regarding the density of buoyancy terms in the equation of motion.

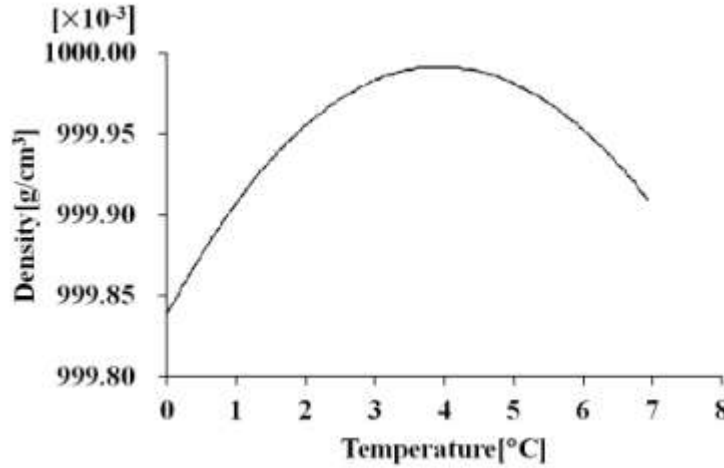


Fig.2 Relationship between water density and temperature by Fujii's expression

### 2.4 Phase Change Solutions and Bridging Time Judgment Method

In this analysis, we used the single-domain calculation model and incorporated the latent heat into the specific heat to solve phase change. Fig.3 shows the relationship between equivalent specific heat and temperature. We assumed that there is a phase change zone (PCZ) in which phase change would occur and the latent heat was incorporated to specific heat at the phase change zone. Equation is shown as the following:

$$c_{ph} = \frac{c_{p,s} + c_{p,l}}{2} + \frac{L}{\Delta T} \quad (10)$$

Where,  $c_{ph}$  represents the incorporated specific heat,  $c_{p,s}$  and  $c_{p,l}$  represent specific heat of the solid and liquid phases respectively.

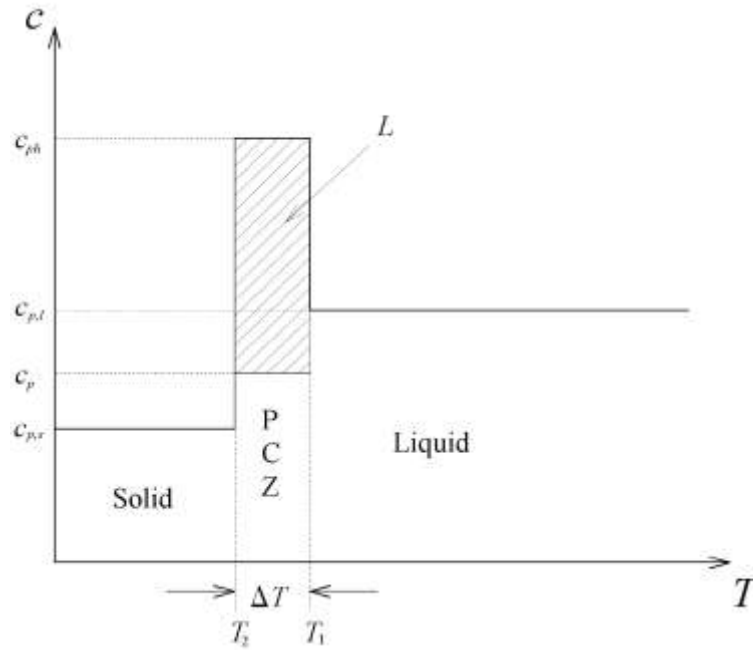


Fig.3 Relationship between equivalent specific heat and temperature.

Additionally, the temperature at each grid is being observed and the velocity at the grid will be set to 0 when its temperature becomes lower than or equals to the solidification temperature  $T_{sp}$ .

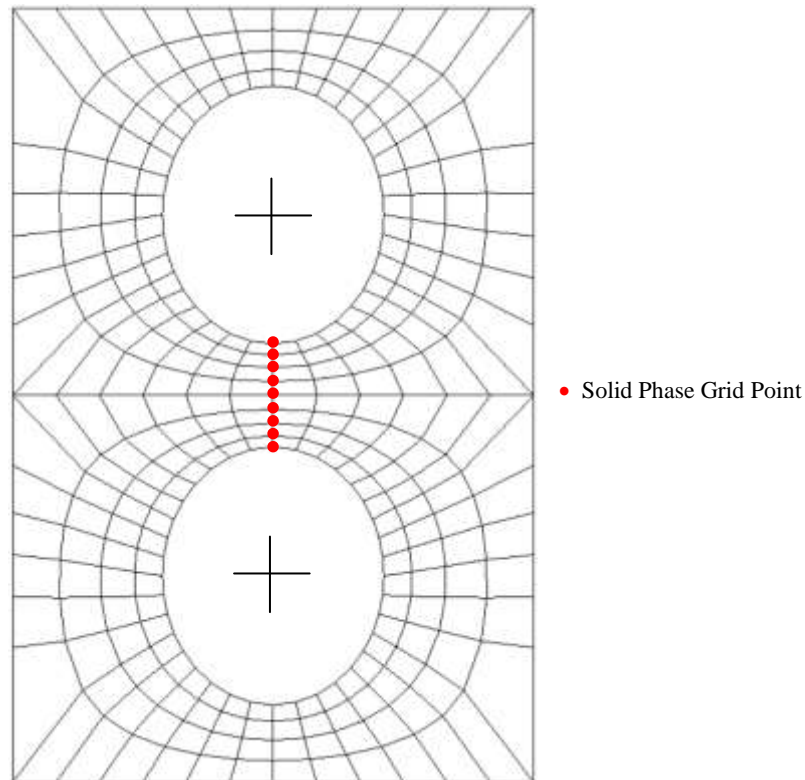


Fig. 4 Judgment method of bridging time.

Each grid point on the physical plane is shown as Fig.4.  $\eta$ -axis is the circumferential direction of the tube and  $\xi$ -axis is the radially direction from the centre of the tube. As mentioned previously, temperature at each grid is being observed. The grid will be judged as liquid if its temperature is higher than the solidification temperature  $T_{sp}$ , otherwise, it will be judged as solid. We focused on each of  $\eta$  grid line from one tube wall to the other and the moment of time will be judged as the bridging time if there appears even just one  $\eta$  line with which all of the grid points on it are judged as solid. Similarly, this method could also be applied to the case when centres of the two tubes are not on the same line in the vertical direction.

2.5 Experimental Apparatus and Method

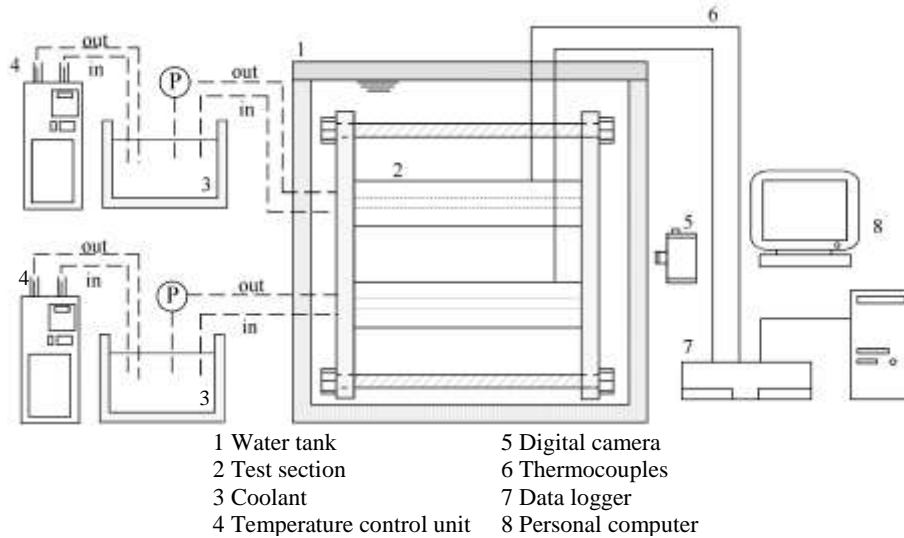


Fig.5 Schematic diagram of experimental apparatus.

Schematic diagram of the experimental apparatus is shown as Fig.5. Roughly, the experimental apparatus could be divided into the test section, thermostatic circulating unit and temperature control unit. Two elliptical tubes which are 190mm in length and made by circular copper pipes were used as the heat transfer tubes. Ellipticity  $\alpha$  of the elliptical tube is 0.85. In addition, inclined angle between the major axis of elliptical tube and the vertical direction was named  $\varphi_g$ . We called it horizontal type when  $\varphi_g = 90^\circ$  and vertical type when  $\varphi_g = 0^\circ$ .

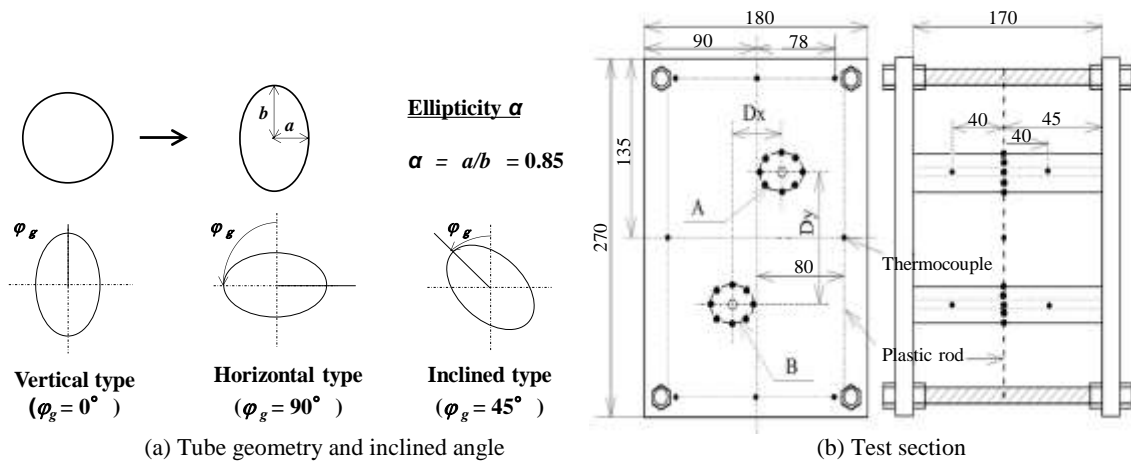
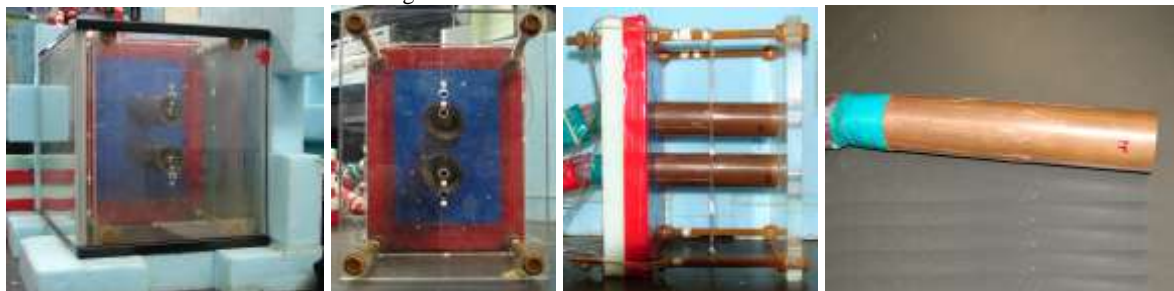


Fig.6 Details of the heat transfer tube and test section.



(a) Experimental water tank (b) Test section (Front view) (c) Test section (Side view) (d) Elliptic copper tube  
Fig.7 Photographs of test section.

Fig.6 (a) shows the geometry and inclined angle of the heat transfer tube, Fig.6 (b) shows the details of the test section and Fig.7 are photographs of the test section. Test area is 270 mm in height, 180 mm in width and 170 mm in depth. In order to prevent the loss of heat, the heat insulation material was covered around water tank. T type thermocouples in a diameter of 0.2 mm were used to the measure the temperature of set points. Finally, photos of the solidification interface shape were taken at predetermined time intervals from the front side of test area. The analysis and experimental results were evaluated by using freezing fraction which was defined as the following:

$$\text{Freezing fraction} = \frac{A_s}{A_c} \tag{11}$$

Where,  $A_c$  and  $A_s$  represent the cross-sectional area of heat transfer tube and generated ice respectively.

### 3. RESULTS AND DISCUSSIONS

The results we will be discussed hereafter are all in two dimensions with the water tank size or analysis area of 180 mm in width and 270 mm in height except special instructions. And also the outer diameter of the heat transfer circular tube is 40 mm or elliptical tube of the same circumferential length with the ellipticity of 0.85 as described above.

#### 3.1 Validity of Present Numerical Analysis

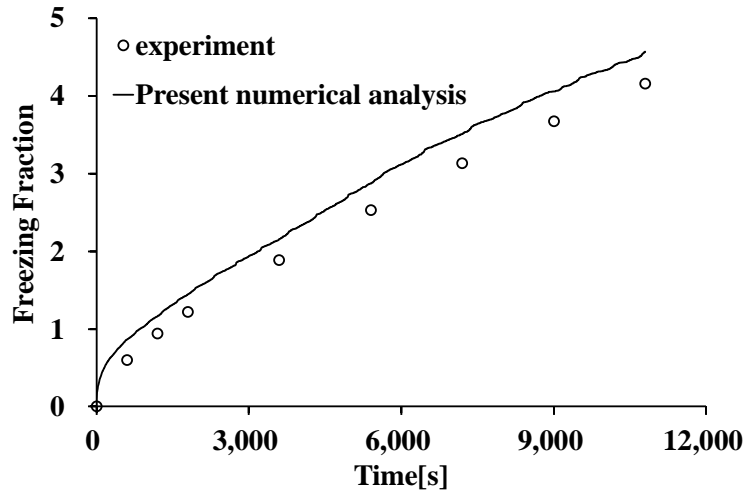


Fig.8 Comparison of freezing fraction by analysis and experiment for two elliptical tubes.  
( $D_x = 0$  mm,  $D_y = 80$  mm,  $\varphi_{g1} = \varphi_{g2} = 90^\circ$ ,  $T_{ini} = 4.0$  °C,  $T_{w,1} = T_{w,2} = -10$  °C)

In order to verify validity of the present numerical analysis, we compared analytical results with the experimental results in freezing fraction, transient average temperature distribution of water and freezing front contour at the same conditions.

Comparison of freezing fraction was shown as in Fig.8. Solid line represents the analytical result and plot points represent experimental result. We found that both of the results were growing with time in the same trend. We can also find that the freezing fraction by analysis was a little higher than that of the experiment. The reason is that there existed heat loss more or less at the experiment in reality. Though we covered the heat insulation material around the water tank, it cannot completely avoid the heat loss.

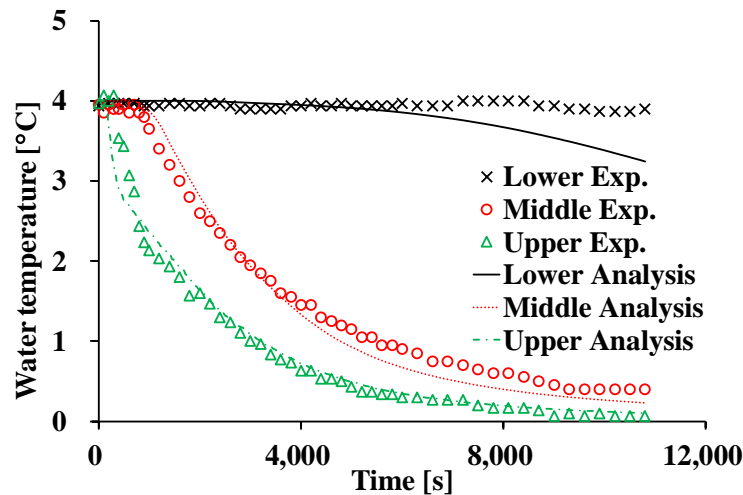


Fig.9 Transient average temperature distribution of water for two elliptical tubes.  
( $D_x = 0$  mm,  $D_y = 80$  mm,  $\varphi_{g1} = \varphi_{g2} = 90^\circ$ ,  $T_{ini} = 4.0$  °C,  $T_{w,1} = T_{w,2} = -10$  °C)

Results in Fig.9 are the transient average temperature distribution of water by analysis and experiment. The Lower Exp., Middle Exp. and Upper Exp. represent the average temperature of the lower three points, the middle two points and the upper three points respectively, which were shown as in Fig.6 (b). And as for the items in analysis, they represent the average temperature of all the grids at the upper part, two points on each side of the middle side and all the grids at the lower part respectively. We can see that the temperature of upper side by experiment was higher than the initial water temperature because of the heat flow from outside. In addition, we also found that there was almost no temperature change with time and a relatively higher temperature of water was accumulating at the lower side all over time. However, the temperature of the middle and the upper sides were dropping over time rapidly.

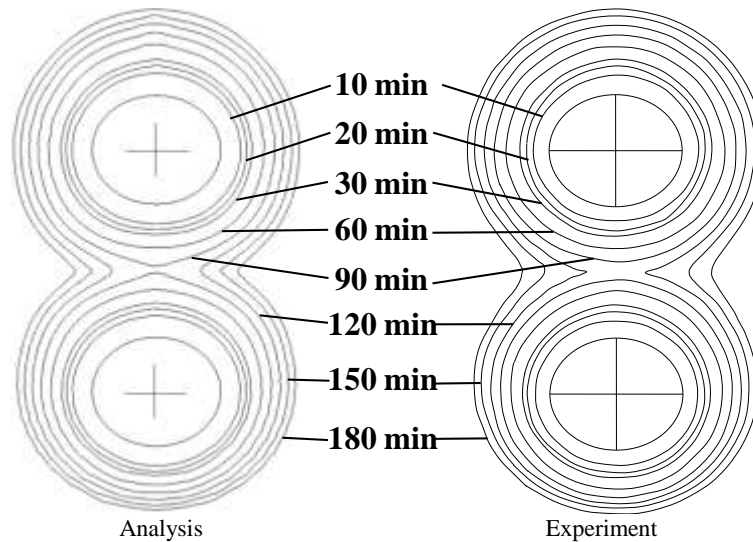


Fig.10 Comparison of freezing front contour by analysis and experiment for two elliptical tubes.  
 ( $D_x = 0$  mm,  $D_y = 80$  mm,  $\phi_{g1} = \phi_{g2} = 90^\circ$ ,  $T_{ini} = 4.0$  °C,  $T_{w,1} = T_{w,2} = -10$  °C )

Figure10 shows the comparison of freezing front contours by analysis and experiment. We found that the freezing fraction of upper tube was slightly thicker compared with the lower tube both in the results of analysis and experiment because of the rising cold flow. Through the above comparison, we found that the qualitative features of the freezing fraction, temperature distribution and freezing front contour by analysis were reasonable compared with the results of experiment though there were some differences.

### 3.2 Bridging Phenomenon

Figure11 are isotherms and velocity vectors by analysis at initial water temperature of  $T_{ini} = 4.0$  °C and Fig.12 are results at initial water temperature of  $T_{ini} = 7.0$  °C. in both of the figures: (a) is the result of 1000 s after analysis beginning; (b) is just before the ice bridging and (c) is immediately after the ice bridging.

In both Fig.11 and Fig.12, We found that the temperature gradient near the bridged ice surface became small and thus produced a faster freezing area because it can easily absorb heat from the surroundings. Furthermore, the flow was completely separated by the binding of ice after bridging and compared with other part, the temperature between the two tubes was lower with a weak flow so that the growth of ice could be higher in a short period immediately after bridging. In addition, the rising flow was generating all over the time and became weaker with time going by when the initial water temperature was 4 °C in both Fig.11. However, as shown in Fig.12, downward flow was first generated and then gradually transformed into the raising flow with the deposition of water at the bottom side when the initial water temperature was 7 °C and the reason could be considered as the characteristic of density inversion.

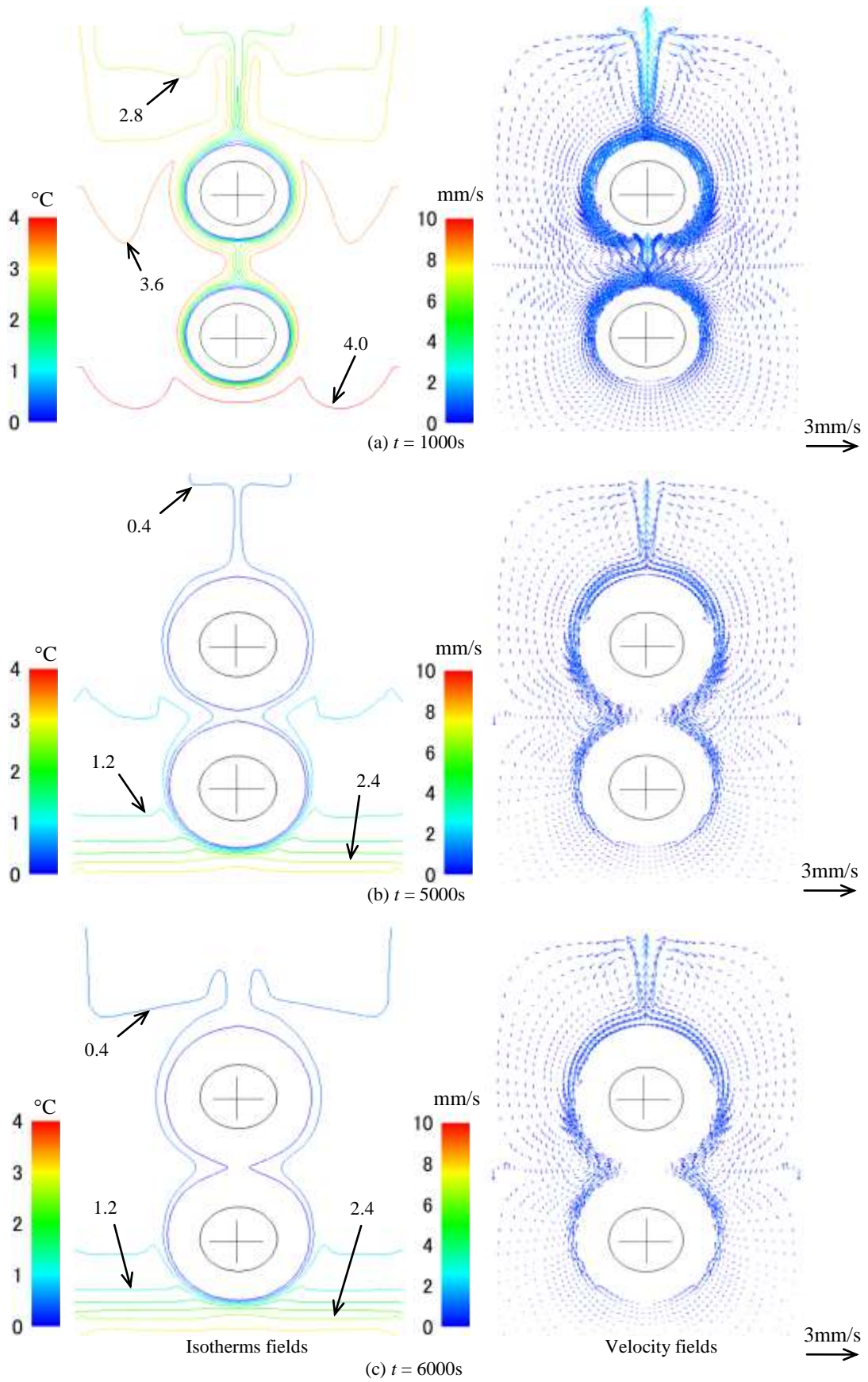


Fig.11 Isotherms and velocity vectors. ( $D_x = 0$  mm,  $D_y = 80$  mm,  $\varphi_{g1} = \varphi_{g2} = 90^\circ$ ,  $T_{ini} = 4.0$  °C,  $T_{w,1} = T_{w,2} = -10$  °C)

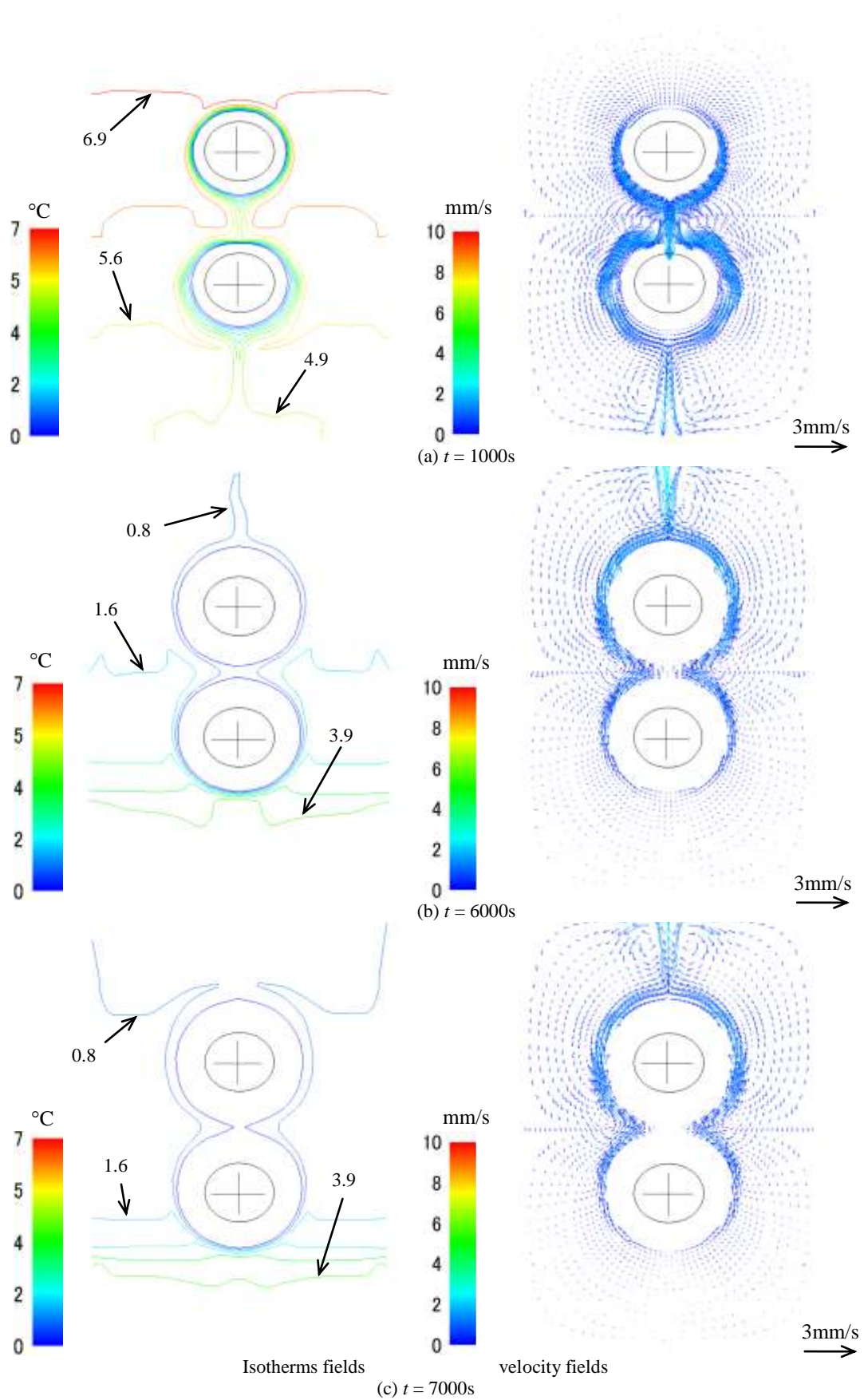


Fig.12 Isotherms and velocity vectors. ( $D_x = 0\text{ mm}$ ,  $D_y = 80\text{ mm}$ ,  $\varphi_{g1} = \varphi_{g2} = 90^\circ$ ,  $T_{ini} = 7.0\text{ }^\circ\text{C}$ ,  $T_{w,1} = T_{w,2} = -10\text{ }^\circ\text{C}$ )

Fig.13 shows the simulated transient circumferential length of ice layer by analysis and the line appears as a serrated shape is due to the influence of grid shape in calculation. We know that the frozen interface will become to the heat transfer surface at the temperature of 0 °C and the heat transfer area in three dimensions will be proportional to the circumferential length of the freezing interface in a two-dimensional analysis. We found that though the transient circumferential length of ice layer increased a little after bridging, it was no significant change, which would lead to the reducing of heat storage efficiency. Therefore, it is necessary to avoid ice bridging in order to improve heat storage efficiency. So it is important to investigate the bridging time.

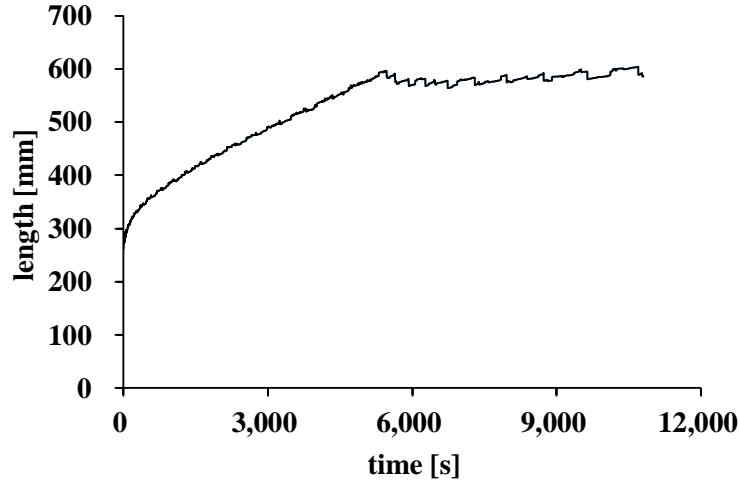


Fig.13 Transient circumferential length of ice layer. ( $D_x = 0$  mm,  $D_y = 80$  mm,  $\varphi_{g1} = \varphi_{g2} = 90^\circ$ ,  $T_{ini} = 4.0$  °C,  $T_{w,1} = T_{w,2} = -10$  °C)

### 3.3 Prediction of Bridging Time

As we discussed above, we know that heat storage efficiency will be reduced because the growth of circumferential length become moderate after bridging.

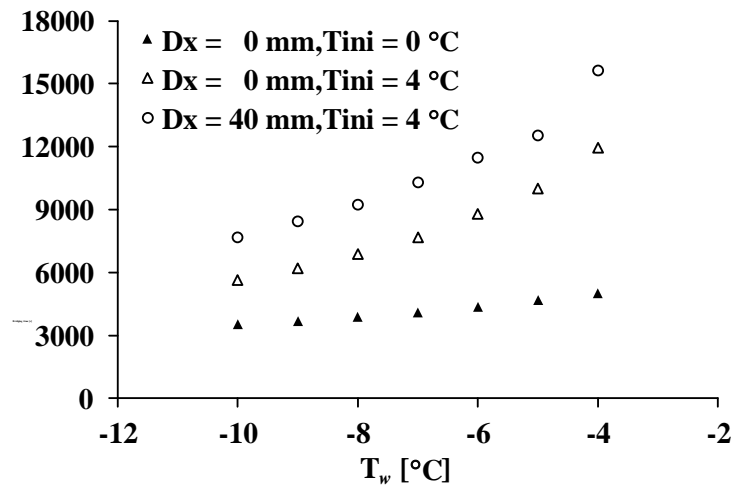


Fig.14 Relationship between bridging time and tube wall temperature. ( $D_y = 80$  mm,  $\varphi_{g1} = \varphi_{g2} = 90^\circ$ )

Figure14 shows the relationship between bridging time and temperature of tube wall. Firstly, we can see from the figure that the bridging time grows linearly with the increasing temperature of tube wall when the initial temperature of water is 0 °C at the condition of  $D_x = 0$  mm. We considered that when the initial temperature of water is 0 °C, there will be no natural convection around the tube and the mode of heat transfer will be heat conduction, so the growing of ice will be decided by the temperature of tube wall. Secondly, when the initial temperature of water is 4 °C, we can know that the increment of bridging time becomes bigger and bigger with the increasing temperature of tube wall compared with that of the initial temperature water is 0 °C at the condition of  $D_x = 0$  mm. We considered that when the temperature difference of initial water and heat transfer tube wall is big, the water will be cooled rapidly and then the influence of convection will become stronger; otherwise, the influence of convection becomes weak and the main mode of heat transfer will be turned into heat conduction. Thirdly, we can also find that the bridging time grows with the increasing temperature of tube wall not linearly but as a tendency of quadratic function both in the cases of  $D_x = 0$  mm and 40 mm at the initial water temperature of 4 °C. As for the reason, it can be considered that the cooled water around the tube wall will flow into the upper side because the density of water becomes highest at 4 °C and we can also see the rising flows in Fig.11, as a result, the energy which should be used to generate ice would be firstly used to cool the water in the container. Finally, it is also found that the freezing time has similar characteristics when changing the horizontal distance between the two tubes.



- [9]. T.J.Scanlon and M.T.Stickland, "A numerical analysis of buoyancy-driven melting and freezing," *Int. J. Heat Mass Transfer*, Vol. 47, No. 3, pp.429-436, 2004.
- [10]. G. Casano, S. Piva., "Experimental and numerical investigation of the steady periodic solid-liquid phase-change heat transfer," *Int J Heat Mass Transfer*, Vol. 45, No. 20, pp. 4181- 4190, 2002.
- [11]. M. Longeon, A. Soupart, J. Fourmigué, A. Bruch, P., "Marty Experimental and numerical study of annular PCM storage in the presence of natural convection," *Appl Energy*, Vol.112, pp. 175-184, 2013.
- [12]. Y. Kozak, T. Rozenfeld, and G. Ziskind, "Close-contact melting in vertical annular enclosures with a non-isothermal base: theoretical modeling and application to thermal storage," *Int J Heat Mass Transfer*, Vol.72, pp. 114-127, 2014.
- [13]. Japan Society of Mechanical Engineers Data Book, *Heat Transfer 5th Edition* (in Japanese), Japan Society of Mechanical Engineers, pp.291-293, 2009.
- [14]. T. Fujii, et al., *Advance of Heat Transfer Engineering 3* (in Japanese). Yokendo, PP.65-68, 1974.